

Cobalt Decoration on Cu₂O Photocatalyst via Electrodeposition for Enhanced Methylene Blue Degradation

Bella Pricilya¹, Nindys Aprillia¹, Shyla Noureen Zahra², Fergie Wulandari², Faisal Abnisa³

¹Department of Chemistry, Faculty of Mathematics and Natural Science, Universitas Negeri Jakarta, Jl. Rawamangun Muka, Jakarta 13220, Indonesia

²The Center for Science Innovation Arva Building, Jl. RP. Soeroso, Jakarta 10350, Indonesia

³Department of Chemical and Material Engineering, Faculty of Engineering, King Abdulaziz University, Rabigh 21911, Saudi Arabia

*Corresponding author: bellapricilya26@gmail.com

Received

10 September 2025

Received in revised form

15 October 2025

Accepted

21 October 2025

Published online

31 October 2025

DOI

<https://doi.org/10.56425/cma.v4i3.122>



© 2023 The author(s). Original content from this work may be used under the terms of the [Creative Commons Attribution 4.0 International License](https://creativecommons.org/licenses/by/4.0/).

Abstract

Cuprous oxide (Cu₂O) is a promising material for photocatalysis due to its narrow bandgap, cost-effectiveness, and non-toxicity. However, its practical application is hindered by the rapid recombination of electron-hole pairs and low stability. This study addresses these limitations by decorating Cu₂O film with a cobalt (Co) cocatalyst. The Cu₂O/Co film was successfully synthesized on indium tin oxide (ITO) substrate through electrodeposition. Characterisation results confirmed the presence of small, agglomerated Co deposits that scattered on Cu₂O grain boundaries. Electrochemical impedance spectroscopy showed that Cu₂O/Co exhibited a charge transfer resistance of 21.94 Ω, which is lower compared to Cu₂O at 24.16 Ω. This indicates that the addition of Co enhances interfacial charge transfer kinetics. Photodegradation test of Cu₂O with Co then revealed a higher degradation efficiency of 76.51% than that of Cu₂O film at 67.55%, highlighting the potential of Co as a cocatalyst for Cu₂O.

Keywords: cobalt cocatalyst, Cu₂O, electrodeposition, methylene blue, photodegradation

1. Introduction

Methylene blue (MB) is a highly toxic cationic dye widely used in the textile dyeing industry, including batik production [1]. During the MB dyeing process, only about 5% of the dye is used, while the remainder is discarded. The high toxicity of this waste, despite the small amount used, makes it a significant environmental hazard. This dye can cause permanent damage to human eyes and aquatic animals, cancer, jaundice, cell mutation, vomiting, and cyanosis [2]. Various methods have been developed for MB wastewater treatment, including coagulation [3], nanofiltration [4,5], phytoremediation [6,7], adsorption [8], and electrocoating [9,10]. In recent decades, photodegradation has been the most widely developed

method because it can efficiently degrade MB waste. The material photocatalysts used in this process can be synthesized through various techniques, and among these methods, electrodeposition is highly promising. This method offers several advantages such as low synthesis temperature, low production costs, and high product purity [11]. Additionally, electrodeposition allows control over the stoichiometry, thickness, and microstructure of the resulting film by adjusting the deposition parameters.

Cuprous oxide (Cu₂O) is a nanostructured oxide classified as a “p-type” semiconductor material due to the presence of copper electron vacancies in its crystal structure, resulting in a low bandgap value of approximately 1.9-2.17 eV [12]. This characteristic makes Cu₂O a highly photoactive material in the visible light

region, suitable for both photoelectrochemical and photovoltaic applications [13]. This material has great potential for use as a catalyst in the photodegradation of dyes such as MB, as it is a low-cost, readily available, and non-toxic catalyst [14]. However, a drawback of Cu_2O is that its electron-hole pairs are prone to recombination, resulting in low quantum efficiency [15]. Pure Cu_2O nanoparticles often exhibit limited photocatalytic efficiency. A significant factor contributing to this low activity is self-oxidation. The resulting species forms a passivating layer on the nanoparticle surface, which blocks incident light leading to a rapid decrease in performance [16]. Therefore, alternatives are needed to enhance the efficiency of utilizing the electron-hole pairs generated by light.

The degradation of MB dye, a persistent pollutant in the environment, remains a significant global challenge. While photocatalytic degradation using Cu_2O nanoparticles has emerged as a promising solution, its practical application is often hindered by low stability and rapid recombination of charge carriers. To address these limitations, the addition of metal cocatalysts such as Au, Pt, Zn, Co, and Ni has been studied to improve the stability of Cu_2O nanoparticles [17]. In this study, a cobalt (Co) cocatalyst was used because of its comparable ability to precious metal-based catalysts, cost-effectiveness, and ability to improve the stability of Cu_2O [18]. The dispersed Co on the Cu_2O particles can act as an electron trap, creating a local electric field that supports charge separation and reduces the likelihood of recombination [11]. Additionally, the formation of a metal-semiconductor interface, a Schottky junction, between Co and Cu_2O accelerates electron transfer to the reaction sites on the surface, enhancing the efficiency of redox reactions [19]. The presence of Co can also enhance the structural stability of Cu_2O by inhibiting the transformation of Cu^+ into Cu^{2+} , which is detrimental. In this study, the decoration of Cu_2O with Co was performed using the electrodeposition method to assess its efficiency in degrading MB dye.

2. Materials and Method

2.1 Fabrication of Cu_2O and $\text{Cu}_2\text{O}/\text{Co}$ thin film

The materials used for this research were copper sulfate pentahydrate ($\text{CuSO}_4 \cdot 5\text{H}_2\text{O}$, Merck), lactic acid ($\text{C}_3\text{H}_6\text{O}_3$, Merck), sodium sulfate (Na_2SO_4 , Merck), sodium hydroxide (NaOH, Merck), cobalt(II) sulfate heptahydrate ($\text{CoSO}_4 \cdot 7\text{H}_2\text{O}$, Merck), methylene blue (MB, $\text{C}_{16}\text{H}_{18}\text{ClN}_3\text{S}$, Merck), and indium tin oxide (ITO) as the substrate. Supporting materials such as distilled water and ethanol were also used.

2.2 Fabrication of Cu_2O and $\text{Cu}_2\text{O}/\text{Co}$ thin film

The electrodeposition method used in this study was controlled using CS310 workstation with a three-electrode system, where Ag/AgCl (KCl 3M) was used as the reference electrode, platinum as the counter electrode, and indium tin oxide (ITO) as the working electrode. Cu_2O was deposited on an ITO substrate that had been repeatedly rinsed with ethanol and distilled water. The deposition process was carried out at a constant potential of -0.3 V for 1 h at 60°C. A solution of 0.05 M $\text{CuSO}_4 \cdot 5\text{H}_2\text{O}$ was used as the electrolyte. The pH of the solution was then adjusted to pH 10.00 using 10 M NaOH solution. Surface modification of Cu_2O with cobalt as a cocatalyst was performed using a constant potential of -1.25 V. Cobalt was deposited by immersing the Cu_2O film into a 0.1 M $\text{CoSO}_4 \cdot 7\text{H}_2\text{O}$ solution at room temperature for 15 seconds.

2.3 Characterization

The synthesized samples were characterized to determine their structural, morphological, elemental, and optical properties. The crystalline phases were identified by X-Ray diffraction (XRD). Morphological analysis was examined using scanning electron microscope (SEM), while elemental composition analysis was verified using energy dispersive X-Ray fluorescence (EDXRF). The optical properties of the films were determined using Tauc-plot curves from reflectance spectra measured by sphere reflectance integrated-UV-Vis (UV-Vis ISR).

2.4 Electrochemical measurements

Photoelectrochemical measurements were conducted using electrochemical impedance spectroscopy (EIS), and linear sweep voltammetry (LSV) techniques. All measurements were performed using a standard three-electrode system and controlled using a Corrtest CS310 workstation under simulated solar irradiation (AM 1.5 G). EIS measurements were performed in the frequency range between 100 kHz and 0.1 Hz. The photocurrent was analyzed using LSV at a bias voltage between -1 V and 1.5 V against Ag/AgCl (3 M KCl) at room temperature, with scan rate of 50 mV/s.

2.5 Photodegradation study

The photocatalytic activity of the samples was evaluated by the degradation of MB solution under visible light irradiation. Data were collected at 5-min intervals for the first 60 min, then at 10-min intervals up to 120 min. The concentrations were monitored using UV-VIS spectrophotometer. The degradation efficiency was calculated using Equation 1.

$$\frac{C_0 - C}{C_0} \times 100\% \quad (1)$$

Where C_0 represents the initial concentration and C denotes the concentration measured at specified irradiation times.

3. Results and Discussion

3.1 Structure, phase, and morphology

The XRD patterns of the samples are shown in Fig 1. The phase of Cu_2O was confirmed present in both Cu_2O and $\text{Cu}_2\text{O}/\text{Co}$ according to the COD reference data No. 96-100-0064. The main diffraction peaks were detected at 2θ of 42.51° , 62.87° , and 73.62° , which are associated with the (200), (220), and (311) planes, respectively. The other observed diffraction peaks correspond of the ITO substrate, similar to the XRD reported by Ayeshamariam and Sanjeeviraja [20]. After modification with Co, the diffraction peak on the (220) plane shifted to 62.94° , while the other peaks remained relatively stable. The selective shift observed only on this plane suggests that Co interacts preferentially with certain crystal facets, possibly due to variations in surface energy and atomic arrangement. Despite the peak shift, no new diffraction peaks were observed, confirming that the fundamental cubic structure of Cu_2O remains unchanged. This shift of the (220) diffraction peak toward a higher angle indicates the presence of local lattice strain due to the deposition of Co cocatalyst on the Cu_2O surface, without altering the overall crystal structure of Cu_2O [20]. The undetectable peak of the Co metal phase diffraction is likely due to the low spectrum intensity of Co relative to Cu_2O and its very fine particle distribution, making it difficult to distinguish from the Cu_2O pattern [21]. Overall, the XRD results indicate that the addition of Co does not cause a change in the main phase of Cu_2O , but it can influence the surface structure and local microstrain, which has the potential to enhance the electrochemical and photocatalytic characteristics of the material, as reported in a similar system by [22].

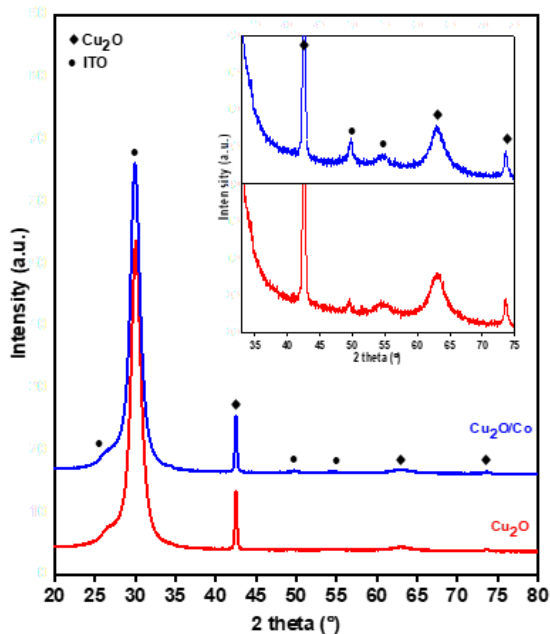


Figure 1. XRD diffractograms of Cu_2O and $\text{Cu}_2\text{O}/\text{Co}$.

SEM micrographs in Fig 2 show the morphology of Cu_2O and $\text{Cu}_2\text{O}/\text{Co}$ synthesized via electrodeposition. The surface morphology of Cu_2O shows grains with clearly defined grain boundaries and relatively uniform sizes, with an average grain size of $2.28 \mu\text{m}$. The addition of the Co cocatalyst to Cu_2O shows a different morphology, where small particles scattered on the grain surface, forming agglomerates. In transition metal cocatalysts such as Co, the particles are more stable when they adhere in groups rather than being evenly distributed across the entire surface, as shown by the SEM images [23,24]. The distribution of Co particles is not completely homogeneous but is localized in certain areas, particularly around grain boundaries.

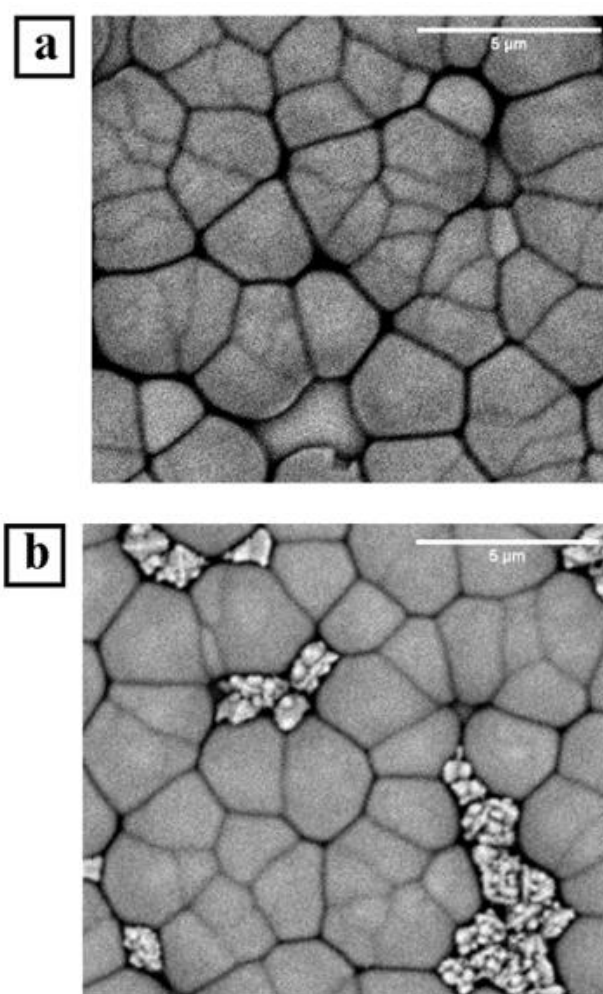


Figure 2. SEM micrographs of the (a) Cu_2O and (b) $\text{Cu}_2\text{O}/\text{Co}$.

The characterization of chemical element content was performed using XRF. Based on Table 1, it was observed that sample Cu_2O shows no impurities, while sample $\text{Cu}_2\text{O}/\text{Co}$ detected the presence of Co at 2.586% with Cu still being the dominant element at 97.414%. The presence of Co proves that the Co deposition process was successful.

Although the detected Co content is relatively small, this value is sufficient to indicate that Co is successfully bound to the Cu_2O surface without forming a significantly separate cobalt oxide phase. These results are consistent with the study [14] which reported that the addition of small amounts of Co to Cu_2O can enhance photocatalytic activity without disrupting the Cu_2O phase structure. Thus, the XRF results confirm that the presence of Co is not a contaminant but a cocatalyst incorporated into Cu_2O to enhance photocatalytic efficiency.

Table 1. Chemical elements of Cu_2O and $\text{Cu}_2\text{O}/\text{Co}$.

Sample	Composition	
	Cu (%)	Co (%)
Cu_2O	99.987	0.0
$\text{Cu}_2\text{O}/\text{Co}$	97.414	2.586

3.2 Electrochemical impedance analysis

Electrochemical impedance spectroscopy (EIS) measurements and Nyquist plots obtained for Cu_2O and $\text{Cu}_2\text{O}/\text{Co}$ are presented in Fig 3. The impedance spectra were fitted using an equivalent circuit model to obtain the bulk resistance (R_s) and charge transfer resistance (R_{ct}) values. The Nyquist plots show a characteristic semicircular shape, where the diameter of the semicircle represents the R_{ct} value at the interface between the photocatalyst and the electrolyte [20]. As shown in the Fig 3, $\text{Cu}_2\text{O}/\text{Co}$ has a smaller semicircular diameter compared to pure Cu_2O . Quantitatively, the R_{ct} value for $\text{Cu}_2\text{O}/\text{Co}$ is 21.94Ω , lower than that of Cu_2O at 24.16Ω . This decrease in charge transfer resistance indicates that the addition of Co as a cocatalyst enhances the interfacial charge transfer kinetics [22], resulting in more effective charge separation on Cu_2O as the primary photocatalyst [23]. This improvement is primarily attributed to the role of Co as a cocatalyst in facilitating interfacial charge transfer, as evidenced by the lower R_{ct} value. However, the increase in the R_s value indicates that the overall bulk conductivity of $\text{Cu}_2\text{O}/\text{Co}$ does not experience a significant increase, suggesting that Co plays a more dominant role at the interface level rather than in enhancing the intrinsic conductivity of the bulk material.

The estimated electrochemically active surface area (ECSA) was calculated using the Equation 2, where C_{dl} represents the electrochemical double-layer capacitance and C_s is the specific capacitance of the material per unit area with the value of 0.001758 F/cm^2 [20].

$$ECSA = \frac{C_{dl}}{C_s} \quad (2)$$

The ECSA value for $\text{Cu}_2\text{O}/\text{Co}$ reaches approximately 1.51 cm^2 , significantly larger than that of Cu_2O at 0.15 cm^2 .

These results indicate an increase in the number of active surface sites and improved electron transfer efficiency at the interface, consistent with the lower R_{ct} value, and confirm that Co enhances the surface kinetics of this photocatalytic system. Although the average particle size of $\text{Cu}_2\text{O}/\text{Co}$ is slightly larger than that of Cu_2O , the ECSA of $\text{Cu}_2\text{O}/\text{Co}$ increases significantly. This indicates that the incorporation of Co enhances the effective electrochemically active surface area through increased surface roughness or porosity, surface decoration by Co deposits, and modifications in surface properties that raise the specific capacitance [33].

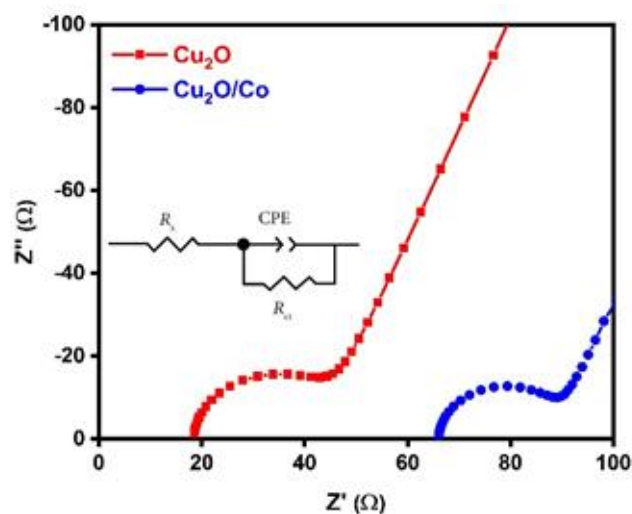


Figure 3. Nyquist plots measured under irradiation for Cu_2O and $\text{Cu}_2\text{O}/\text{Co}$.

3.3 Photoelectrochemical analysis

The photoelectrochemical (PEC) performance of the synthesized samples was evaluated under conditions with and without simulated sunlight irradiation. In Fig 4, Cu_2O exhibits a very small current response in the dark, indicating that the generated electric current is influenced by light irradiation. Under illuminated conditions, the absorbed photon energy triggers electron excitation from the valence band to the conduction band, thereby generating electron-hole pairs that contribute to the generated photocurrent [24]. Based on the test results, the photocurrent density of Cu_2O reached 4.55 mA/cm^2 at a potential of 0.15 V vs Ag/AgCl .

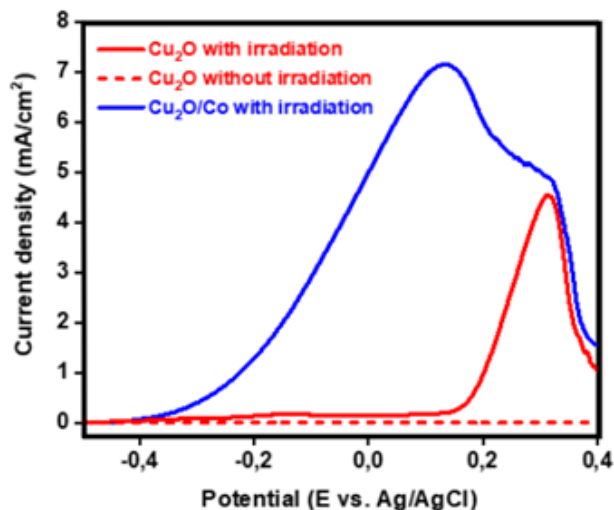


Figure 4. Photocurrent responses without and with irradiation for Cu_2O and $\text{Cu}_2\text{O}/\text{Co}$.

After the deposition of Co cocatalyst, this value increased to $7.15 \text{ mA}/\text{cm}^2$ at a potential of 0.13 V . Additionally, the onset potential of $\text{Cu}_2\text{O}/\text{Co}$ shifted negatively to -0.4 V , compared to 0.15 V for Cu_2O , indicating that the photoelectrocatalytic reaction can occur at a lower potential bias. These results indicate that the addition of Co as a cocatalyst effectively facilitates more efficient charge separation and suppresses electron-hole pair recombination on Cu_2O [20]. The presence of Co also promotes the transfer of light-excited electrons, thereby showing potential to enhancing photocatalytic performance. This is supported by EIS measurement results showing a decrease in R_{ct} values after Co deposition.

3.4 Photocatalytic degradation of Methylene Blue

Figure 6 presents the degradation efficiency of the MB degradation, showing that Cu_2O was able to degrade MB by 67.55%, while $\text{Cu}_2\text{O}/\text{Co}$ increased the degradation by 1.13 times compared to Cu_2O , reaching 76.51%. This increase can be attributed to the synergistic effect between Cu_2O and Co, which facilitates more efficient separation and transfer of charge carriers (electrons and holes) [25].

In the $\text{Cu}_2\text{O}/\text{Co}$ thin film, the presence of Co provides additional active sites that promote the migration of photoexcited electrons, thereby reducing the recombination rate. Better charge separation extends the lifetime of electron-hole pairs and enhances redox reactions with MB pollutants [26]. Additionally, Co can act as a cocatalyst, enhancing the system's reduction capability by forming highly reactive hydroxyl radicals. These $\cdot\text{OH}$ radicals will react with MB, producing

compounds like carbon dioxide, water, and inorganic ions, as shown in the following reaction:

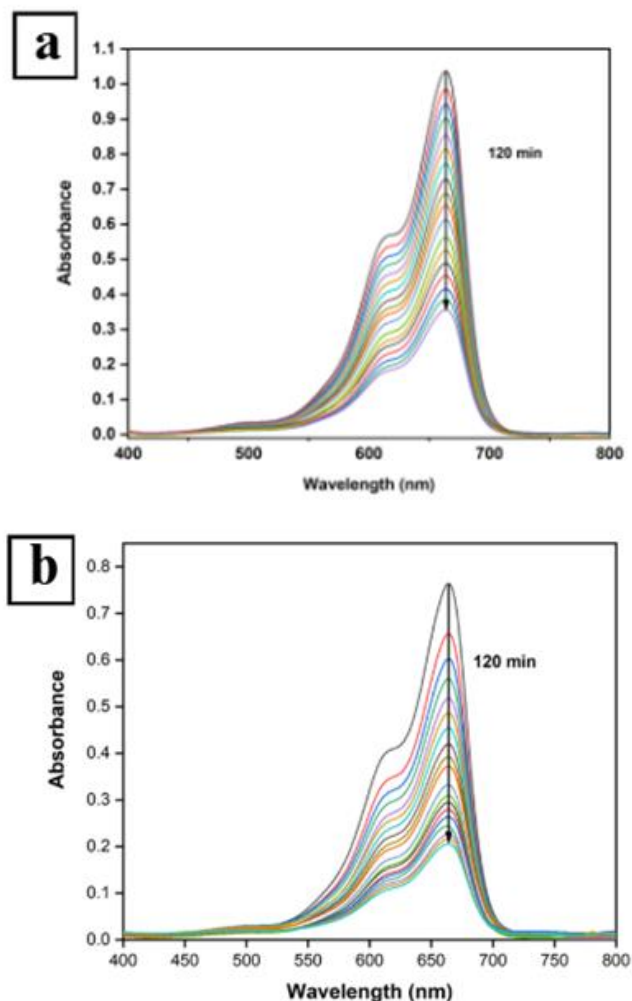
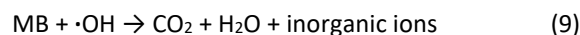
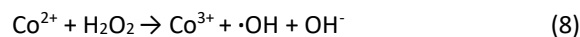
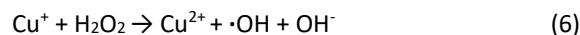
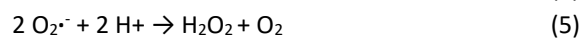


Figure 5. UV-VIS absorbance spectra of (a) Cu_2O and (b) $\text{Cu}_2\text{O}/\text{Co}$.

When a photocatalyst like Cu_2O is exposed to light, electron-hole pairs are formed. To initiate the degradation reaction, electrons must be transferred to the surface and interact with dissolved oxygen, while holes react with water or hydroxide ions to form hydroxyl radicals ($\cdot\text{OH}$) [10]. However, this process can be disrupted by electron-hole recombination within the material before they can react at the surface. A low R_{ct} indicates high charge mobility, meaning more electrons or holes reach the surface and participate in the photocatalytic reaction. The

lower the R_{ct} value, the more efficient the charge transfer to the interface, thereby enhancing hydroxyl formation, which functions to degrade methylene blue.

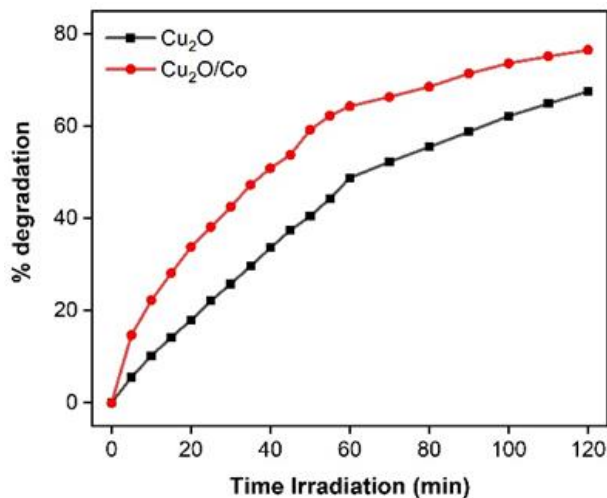


Figure 6. Photodegradation of MB using Cu₂O and Cu₂O/Co.

3.5 Optical analysis

The UV-Vis transmission results were used to estimate the optical bandgap (E_g) of the Cu₂O and Cu₂O/Co thin films. The E_g values were determined by plotting the $(F(R)hv)^2$ against photon energy and extrapolating the linear portion of the plot to its intercept with energy axis, as shown in Fig 7. Using this method, E_g was found to be around 2.00 eV for both samples. The invariance of the band gap may result from the likelihood that Co deposits are present only on the surface as a cocatalyst without substantially substituting Cu ions within the Cu₂O crystal lattice [31]. Consequently, the valance band and structures of Cu₂O are preserved. Therefore, although the addition of Co enhances photocatalytic activity by improving charge separation and electron transfer, its effect is not reflected in a modification of the band gap of Cu₂O. Although a change in band gap can influence photocatalytic activity by affecting light absorption, it is not the sole determining factor. Photocatalytic performance is more strongly governed by charge separation efficiency, generation of reaction of reactive oxygen species (ROS), and electron transfer kinetics. Therefore, even if the band gap of Cu₂O remains nearly unchanged after the deposition of Co, the photocatalytic activity can still be significantly enhanced due to improved charge separation and interfacial reaction.

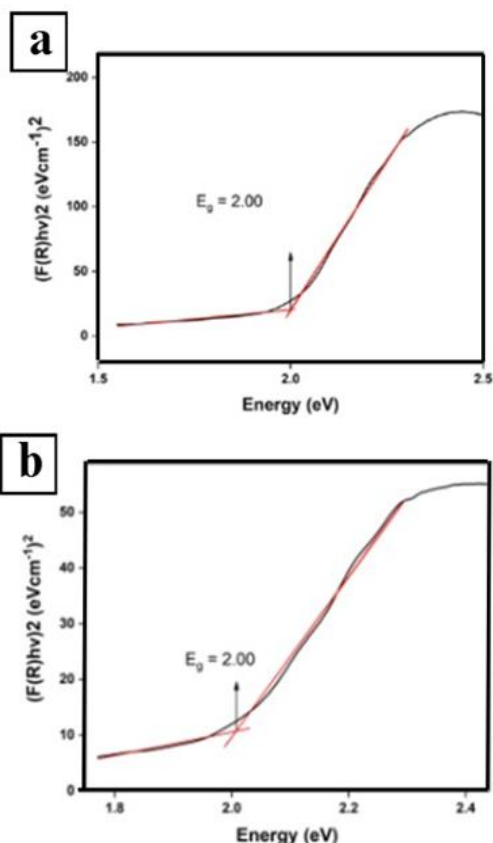


Figure 7. Bandgap values of (a) Cu₂O and (b) Cu₂O/Co.

4. Conclusion

Cu₂O photocatalysts with the addition of Co cocatalyst were successfully synthesized via electrodeposition on ITO substrates for methylene blue (MB) degradation. Degradation experiments showed that the presence of Co deposits in Cu₂O increased the degradation efficiency from 67.55% to 76.51% under visible light irradiation. Impedance data showed that the Cu₂O/Co film had a lower charge transfer resistance (R_{ct}) compared to pure Cu₂O, namely 21.94 Ω and 24.16 Ω , respectively. This reduction indicates an increase in charge separation efficiency and mobility on the material surface. Thus, Cu₂O/Co has high potential as an environmentally friendly photocatalyst for organic wastewater treatment applications.

Author contributions

Bella Pricilya: Investigation, Formal analysis, Writing-original draft, Visualization. **Nindys Aprillia:** Investigation, Writing-Review and Editing. **Shyla Noureen Zahra:** Visualization, Formal Analysis. **Firgie Wulandari:** Conceptualization, Methodology, Software, Formal Analysis. **Faisal Abnisa:** Supervision, Project Administration.

Conflicts of interest

The authors declare no conflicts of interest.

Acknowledgement

The authors acknowledge that this work was funded by Direktorat Penelitian dan Pengabdian kepada Masyarakat (DPPM) Kemendikisaintek under Penelitian Terapan Luaran Prototipe Scheme 2025 (3/UN39.14/C3/DT.05.00/PT-LP/PL/2025).

References

- [1] Z. Mulushewa, W. T. Dinbore, and Y. Ayele, Removal of methylene blue from textile wastewater using kaolin and zeolite-x synthesized from Ethiopian kaolin, *Environ Anal Health Toxicol*, **36** (2021). <https://doi.org/10.5620/eaht.2021007>.
- [2] B. Y. Patel and H. K. Patel, Current approaches toward the removal of methylene blue dye from synthetic textile effluent using bacterial treated agricultural waste absorbent through statistical design, *Heliyon*, **9** (2023) 9. <https://doi.org/10.1016/j.heliyon.2023.e19857>.
- [3] H. M. Ahmed, M. E. Fawzy, and H. F. Nassar, Effective Chemical Coagulation Treatment Process for Cationic and Anionic Dyes Degradation, *Egypt J Chem*. **65** (2022) 301–310. <https://doi.org/10.21608/ejchem.2022.109537.4993>
- [4] D. Naresh Yadav, K. Anand Kishore, and D. Saroj, A Study on removal of Methylene Blue dye by photocatalysis integrated with nanofiltration using statistical and experimental approaches, *Environmental Technology (United Kingdom)*, **42** (2021) 2968–2981. <https://doi.org/10.1080/09593330.2020.1720303>.
- [5] R. Farhadi, M. A. Aroon, A. Ebrahimian Pirbazari, M. Safarpour, T. Matsuura, and P. Seirafi, Simultaneous separation and degradation of methylene blue by a thin film nanocomposite membrane containing TiO₂/MWCNTs nanophotocatalyst, *Environmental Technology (United Kingdom)*. **44** (2023) 670–685. <https://doi.org/10.1080/09593330.2021.1982019>.
- [6] O. A. Urucu, B. Garosi, and R. A. Musah, Efficient Phytoremediation of Methyl Red and Methylene Blue Dyes from Aqueous Solutions by *Juncus effusus*, *ACS Omega*. **56** (2025). <https://doi.org/10.1021/acsomega.4c07468>.
- [7] Y. Chen, Z. Xiang, D. Wang, J. Kang, and H. Qi, Effective photocatalytic degradation and physical adsorption of methylene blue using cellulose/GO/TiO₂hydrogels, *RSC Adv*. **10** (2020) 23936–23943. <https://doi.org/10.1039/d0ra04509h>
- [8] I. Khan et al., Review on Methylene Blue: Its Properties, Uses, Toxicity and Photodegradation. **73** (2022). <https://doi.org/10.3390/w14020242>.
- [9] S. Budi, D. I. Syafei, Yusmaniar, Q. F. Khasanah, and D. Laxmianti, Electrodeposition of Cu₂O Films at Room Temperature for Methylene Blue Photodegradation, in *Journal of Physics: Conference Series*, Institute of Physics. **43** (2022). <https://doi.org/10.1088/1742-6596/2377/1/012004>.
- [10] W. Zhao et al., Electrodeposition of Cu₂O films and their photoelectrochemical properties, *CrystEngComm*, **13** (2011) 2871–2877, <https://doi.org/10.1039/c0ce00829j>.
- [11] S. Laidoudi et al., “Growth and characterization of electrodeposited Cu₂O thin films,” *Semicond Sci Technol*. **28** (2013), <https://doi.org/10.1088/0268-1242/28/11/115005>.
- [12] E. Arulkumar, S. Thanikaikarasan, and N. Tesfie, “Influence of Deposition Parameters for Cu₂O and CuO Thin Films by Electrodeposition Technique: A Short Review.” **23** (2023). <https://doi.org/10.1155/2023/8987633>.
- [13] S. J. Taher, A. A. Barzinjy, and S. M. Hamad, The Effect of Deposition Time on the Properties of Cu₂O Nanocubes Using an Electrochemical Deposition Method, *J Electron Mater*. **49** (2020) 7532–7540. <https://doi.org/10.1007/s11664-020-08495-y>.
- [14] X. Yu et al., Ag-Cu₂O composite films with enhanced photocatalytic activities for methylene blue degradation: Analysis of the mechanism and the degradation pathways, *J Environ Chem Eng*. **9** (2021) <https://doi.org/10.1016/j.jece.2021.106161>.
- [15] Z. Yang, C. Ma, W. Wang, M. Zhang, X. Hao, and S. Chen, Fabrication of Cu₂O-Ag nanocomposites with enhanced durability and bactericidal activity, *J Colloid Interface Sci*. **557** (2019) 156–167. <https://doi.org/10.1016/j.jcis.2019.09.015>.
- [16] Z. Yang, C. Ma, W. Wang, M. Zhang, X. Hao, and S. Chen, Fabrication of Cu₂O-Ag nanocomposites with enhanced durability and bactericidal activity, *J Colloid Interface Sci*. **357** (2019) 156–167. <https://doi.org/10.1016/j.jcis.2019.09.015>.
- [17] M. G. Sutrisno, Yusmaniar, A. M. Noor, and S. Budi, Electrodeposition of Zn-Doped Cu₂O-Cu/Ni for methylene blue photodegradation, *Journal of Physics: Conference Series*, Institute of Physics. **41** (2023). <https://doi.org/10.1088/1742-6596/2596/1/012017>.
- [18] S. Budi, M. Gladiani Sutrisno, and T. Hadinugrahaningsih, Synergistic enhancement of photocatalytic efficiency and durability in CoNi-decorated Cu₂O/Cu films for superior synthetic dye degradation, *Cleaner Materials*, **12** (2024). <https://doi.org/10.1016/j.clema.2024.100250>.

- [19] F. S. B. Kafi, K. M. D. C. Jayathileka, R. P. Wijesundera, and W. Siripala, Improvement of photovoltaic properties of n-Cu₂O/Au Schottky junctions, *Mater Res Express*. **6** (2019). <https://doi.org/10.1088/2053-1591/ab20b6>.
- [20] A. Ayeshamariam and C. Sanjeeviraja, Study Of Size Controllable Synthesis of Indium Tin Oxide Nanoparticles and Their Different Characterization, **23** (2012) 122–132. <https://doi.org/10.1007/s10832-021-00225-6>.
- [21] G. F. Harrington and J. Santiso, Back-to-Basics tutorial: X-ray diffraction of thin films, *J Electroceram*, **47** (2021) 141–163. <https://doi.org/10.1007/s10832-021-00263-6>.
- [22] F. Conte *et al.*, Effect of Metal Cocatalysts and Operating Conditions on the Product Distribution and the Productivity of the CO₂ Photoreduction, *Ind Eng Chem Res*. **61** (2022) 2963–2972. <https://doi.org/10.1021/acs.iecr.1c02514>.
- [23] S. Noureen Zahra, Fergie Wulandari, Muhammad Raihan Rauf, and A. Arum, Decorating Cu₂O with Copper Metal (Cu) through Facile Electrochemical Deposition for Methylene Blue Degradation, *Chemistry and Materials*. **3** (2024) 71–80. <https://doi.org/10.56425/cma.v3i3.81>.
- [24] D. Peña, A. Griboval-Constant, F. Diehl, V. Lecocq, and A. Y. Khodakov, Agglomeration at the Micrometer Length Scale of Cobalt Nanoparticles in Alumina-Supported Fischer-Tropsch Catalysts in a Slurry Reactor, *ChemCatChem*. **5** (2013) 728–731. <https://doi.org/10.1002/cctc.201200703>.
- [25] B. Liu, X. Zhang, H. Shioyama, T. Mukai, T. Sakai, and Q. Xu, Converting cobalt oxide subunits in cobalt metal-organic framework into agglomerated Co₃O₄ nanoparticles as an electrode material for lithium-ion battery, *J Power Sources*. **195** (2010) 857–861. <https://doi.org/10.1016/j.jpowsour.2009.08.058>.
- [26] M. Ali, R. Maulana, B. Trigoutomo, and A. Mahmud, The effect of Phase Composition on the Photocatalytic Activity of Cu₂O / CuO / Cu Composites for Methylene Blue Photodegradation. **4** (2025) 1–8. <https://doi.org/10.1016/j.cej.2020.124262>.
- [27] X. Meng, C. Zhang, C. Dong, W. Sun, D. Ji, and Y. Ding, Carbon quantum dots assisted strategy to synthesize Co@NC for boosting photocatalytic hydrogen evolution performance of CdS, *Chemical Engineering Journal*. **389** (2019) 124432, 2020. <https://doi.org/10.1016/j.cej.2020.124432>.
- [28] Q. Zhao, W. Yao, C. Huang, Q. Wu, and Q. Xu, “Effective and Durable Co Single Atomic Co- catalysts for Photocatalytic Hydrogen Production Effective and Durable Co Single Atomic Co-catalysts for Photocatalytic Hydrogen Production. **65** (2017). <https://doi.org/10.1021/acsami.7b13566>.
- [29] S. Budi, M. G. Sutrisno, Y. Pratiwi, and N. Yusmaniar, Enhanced photocatalytic activity of CoNi-decorated Zn-doped Cu₂O synthesized by electrodeposition technique, *Mater Adv*. **4** (2023) 1081–1088. <https://doi.org/10.1039/d2ma00916a>.
- [30] I. Akhirudin, S. Budi, and Yusmaniar, Electrodeposition of Zn-doped Cu₂O for the Photodegradation of Methylene Blue, *Journal of Physics*. **78** (2020). <https://doi.org/10.1088/1742-6596/1428/1/012064>.
- [31] Z. Mulushewa, W. T. Dinbore, and Y. Ayele, Removal of methylene blue from textile wastewater using kaolin and zeolite-x synthesized from Ethiopian kaolin, *Environ Anal Health Toxicol*, vol. 36 (2021). <https://doi.org/10.5620/eaht.2021007>.
- [32] Q. Huang, J. Li, and X. Bi, The improvement of hole transport property and optical band gap for amorphous Cu₂O films, *J Alloys Compd*. **647** (2015) 585-589. <https://doi.org/10.1016/j.jallcom.2015.06.147>.
- [33] J. Yiing Loh, J. Jie Foo, F. Ming Yap, H. Liang, W.J. Ong, Unleashing the versatility of porous nanoarchitectures: A voyage for sustainable electrocatalytic water splitting, *Chinese Journal of Catalysis*. **58** (2024). [https://doi.org/10.1016/S1872-2067\(23\)64581-4](https://doi.org/10.1016/S1872-2067(23)64581-4).